

Tunable Photoswitching in Norbornadiene (NBD)/Quadricyclane (QC) – Fullerene Hybrids

Patrick Lorenz,^[a] Florian Wullschläger,^[b] Antonia Rüter,^[a] Bernd Meyer,^[b] and Andreas Hirsch^{*[a]}

In memoriam of Prof. Michael Hanack.

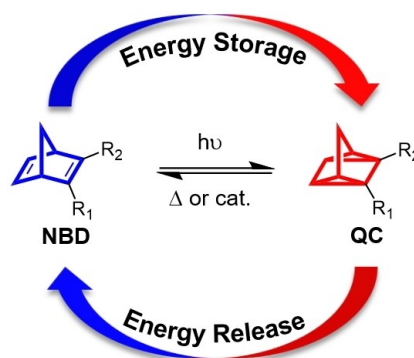
Abstract: With respect to molecular switches, initializing the quadricyclane (QC) to norbornadiene (NBD) back-reaction by light is highly desirable. Our previous publication provided a unique solution for this purpose by utilizing covalently bound C₆₀. In this work, the fundamental processes within these hybrids has been investigated. Variation of the linker unit connecting the NBD/QC moiety with the fullerene core is used as a tool to tune the properties of the resulting hybrids. Utilizing the Prato reaction, two unprecedented NBD/QC –

fullerene hybrids having a long-rigid and a short-rigid linker were synthesized. Molecular dynamics simulations revealed that this results in an average QC–C₆₀ distance of up to 14.2 Å. By comparing the NBD–QC switching of these derivatives with the already established one having a flexible linker, valuable mechanistic insights were gained. Most importantly, spatial convergence of the QC moiety and the fullerene core is inevitable for an efficient back-reaction.

Introduction

The norbornadiene (NBD) – quadricyclane (QC) interconversion couple is a promising concept for the efficient realization of molecular solar thermal (MOST) energy storage systems.^[1] In the course of the corresponding rearrangement, NBD undergoes a light-induced intramolecular cycloaddition to form its highly strained metastable isomer QC. During this process, energy is stored as strain energy in chemical bonds.^[2] Upon demand this energy can be released as thermal energy (Scheme 1).^[3]

Usually, this back-reaction from QC to NBD can be promoted thermally or catalytically. In addition, significant progress has been made lately in the electrochemically triggered energy release.^[4] For a practical implementation of the NBD/QC system into a MOST device, a catalytic energy release is most suitable.^[5] Therefore, considerable effort has been devoted to design efficient catalysts for this reaction.^[6]



Scheme 1. The norbornadiene (NBD) – quadricyclane (QC) interconversion system. Introducing an electron donating group (EDG) and an electron withdrawing group (EWG) in the R₁/R₂ position gives push-pull substituted NBD/QC derivatives.

Next to these established methods there is another one that has not received much attention yet, but brings in the exciting opportunity of selective photoswitching in both directions.^[7] In this particular case, the isomerization of QC to NBD is also induced by light. Such a light-only control is rather rare and in the recent literature only few examples have been reported.

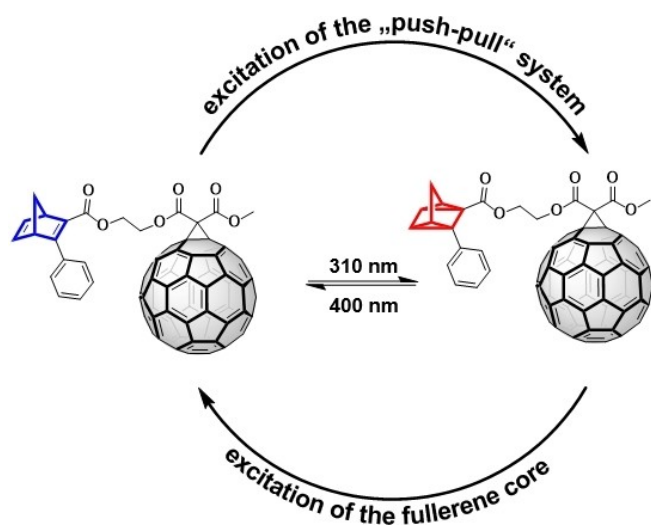
For the application in MOST systems, this type of back-reaction may play a minor role, but it opens up completely new perspectives for the NBD/QC system in the field of molecular switches and information storage. Among these examples, our earlier publication on NBD/QC – fullerene hybrids stands out as the only example where light of a longer wavelength, than the one used for the isomerization of NBD to QC, can be used to promote the back-reaction (Scheme 2).^[7a] This discovery encouraged us to investigate these hybrids as well as the underlying

[a] P. Lorenz, A. Rüter, Prof. Dr. A. Hirsch
Chair of Organic Chemistry II
Friedrich-Alexander-Universität Erlangen-Nürnberg
Nikolaus-Fiebiger-Str. 10, 91058 Erlangen (Germany)
E-mail: andreas.hirsch@fau.de

[b] F. Wullschläger, Prof. Dr. B. Meyer
Interdisciplinary Center for Molecular Materials (ICMM) and
Computer Chemistry Center (CCC)
Friedrich-Alexander-Universität Erlangen-Nürnberg
Nägelsbachstr. 25, 91052 Erlangen (Germany)

Supporting information for this article is available on the WWW under <https://doi.org/10.1002/chem.202102109>

© 2021 The Authors. Chemistry - A European Journal published by Wiley-VCH GmbH. This is an open access article under the terms of the Creative Commons Attribution Non-Commercial NoDerivs License, which permits use and distribution in any medium, provided the original work is properly cited, the use is non-commercial and no modifications or adaptations are made.



Scheme 2. Light-only-controlled interconversion of an NBD/QC – fullerene hybrid as reported in our earlier publication.^[7a] Adapted with permission from P. Lorenz, A. Hirsch, *Chem. Eur. J.* 2020, 26, 5220–5230.

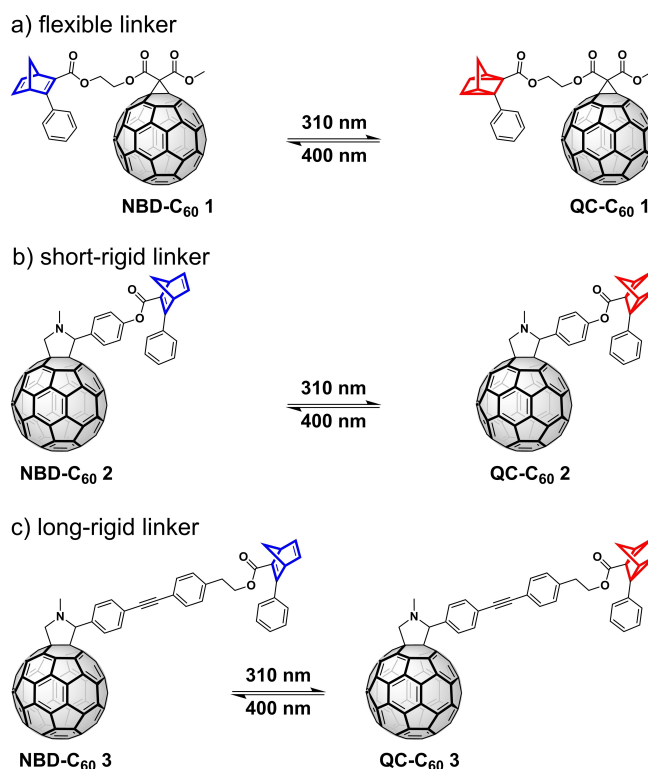
processes during the interconversion in greater detail. Our particular focus of this study is the influence of the rigidity and extension of the linker between the two chromophores.

Herein we describe the design, synthesis, and characterization of two new NBD/QC–C₆₀ hybrids with rigid linkers. By comparing the light-induced reactions NBD to QC at 310 nm and the back-reaction QC to NBD at 400 nm of these derivatives with the already published NBD/QC–C₆₀ 1, which has a flexible linker, valuable insights into the interaction between fullerene core and covalently linked photoswitch are gained. While the nature of the linker has virtually no influence on the NBD to QC isomerization, it has a pronounced effect on the back-reaction. These observations are corroborated by molecular dynamics (MD) simulations and make it possible to shine light on the interconversion process. In particular, close contacts between the fullerene core and the QC moiety seem to be inevitable for promoting the back-reaction to NBD. This not only solidifies our previous assumption that C₆₀ acts as an excited state electron acceptor but also shows that the interaction between QC scaffold and the fullerene core is mainly an intramolecular process.

Results and Discussion

The targeted structures of NBD–C₆₀ 1–3 as well as their corresponding QC derivatives (QC–C₆₀ 1–3) are shown in Scheme 3. Unlike NBD–C₆₀ 1, which has a flexible linker and has already been described in our earlier publication,^[7a] our intention with the two new derivatives is to use rigid linkers to prevent spatial convergence of the fullerene core and the photoswitch as much as possible.

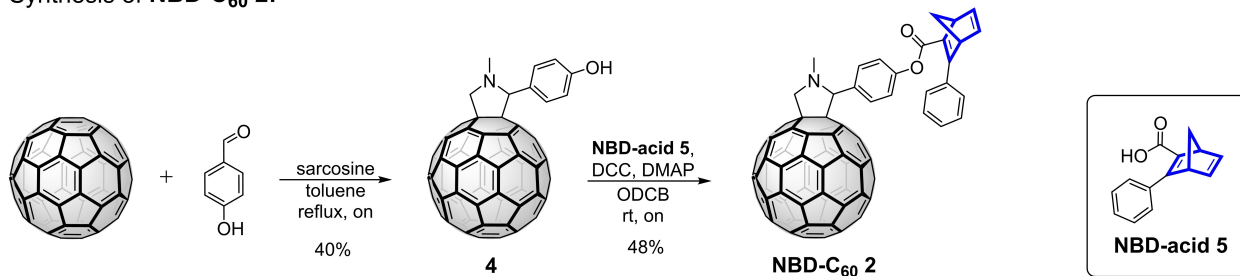
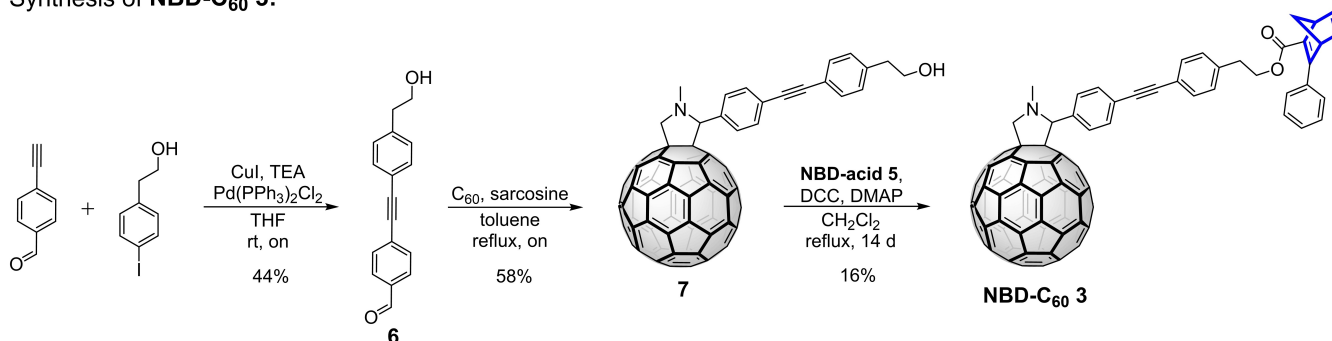
Therefore, we opted to use the Prato reaction to functionalize C₆₀ with rigid spacers carrying hydroxy groups. The hydroxy group serves as an anchor point for the subsequent



Scheme 3. Structures of the NBD/QC – fullerene hybrids investigated in this study. Three different types of linker units between the fullerene core and the photoswitch are used. a) Interconversion of NBD–C₆₀ 1 and QC–C₆₀ 1 with a flexible linker; b) Interconversion of NBD–C₆₀ 2 and QC–C₆₀ 2 with a short-rigid linker; c) Interconversion of NBD–C₆₀ 3 and QC–C₆₀ 3 with a long-rigid linker.

attachment of the NBD moiety via a Steglich esterification. Importantly, in both cases a “push-pull” substituted NBD moiety was used, since this was shown to be inevitable for an efficient isomerization to the corresponding QC derivatives without using a photosensitizer.

The syntheses of NBD–C₆₀ 2 and NBD–C₆₀ 3 are depicted in Scheme 4. NBD–C₆₀ 2 can be synthesized starting from C₆₀ in a straightforward twostep process via the literature known^[8] pyrrolidino fullerene 4. The linker unit between photoswitch and fullerene core in NBD–C₆₀ 2 can be regarded as 4-(N-methylpyrrolidin-2-yl)phenol, which is a short and highly rigid spacer. In the final step of the synthesis, the NBD scaffold is introduced by esterification of NBD–acid 5 with the hydroxy group of compound 4. Using this binding motif, the non-flexible architecture of this hybrid is maintained. The synthesis of NBD–C₆₀ 3 is based on the same strategy. However, a much longer linker was employed, tolane 6 was used in the Prato reaction with sarcosine and C₆₀. The tolane moiety provides a considerably larger distance between the fullerene core and the photoswitch. This allowed for the presence of some flexibility introduced by the ethyl ester which connects the tolane with the NBD moiety. Using this linker, it is ensured that the push-pull systems of NBD–C₆₀ 1 and NBD–C₆₀ 3 both comprise an ethyl ester as electron withdrawing group (EWG), which is an important detail – see below. Both, NBD–C₆₀ 2 and NBD–C₆₀ 3

Synthesis of **NBD-C₆₀ 2**:Synthesis of **NBD-C₆₀ 3**:

Scheme 4. Top: Synthesis of **NBD-C₆₀ 2**; 4-hydroxybenzaldehyde and sarcosine are used in a standard Prato reaction with C_{60} to give the pyrrolidino fullerene **4**, which is successively coupled with **NBD-acid 5** in a Steglich esterification using *N,N'*-dicyclohexylmethanediimine (DCC) and *N,N*-dimethylpyridin-4-amine (DMAP) in *ortho*-dichlorobenzene (ODCB) to give the desired product **NBD-C₆₀ 2**. Bottom: Synthesis of **NBD-C₆₀ 3**; a Sonogashira cross coupling is used to generate the tolane **6**, which is then used together with sarcosine and C_{60} in a Prato reaction to give the pyrrolidino fullerene **7**. The last step in the synthesis of **NBD-C₆₀ 3** is a Steglich esterification with **NBD-acid 5** using DCC and DMAP in CH_2Cl_2 .

were characterized by 1H and ^{13}C NMR spectroscopy as well as mass spectrometry (see Supporting Information). Since the photochemistry of these compounds is of crucial importance, UV/vis absorption spectra of all three hybrids are depicted in Figure 1. In all three cases the typical absorption pattern of fullerene monoadducts is observed including the characteristic absorption band around 430 nm.^[9] Remarkably, no distinct absorption features of the NBD push-pull systems can be

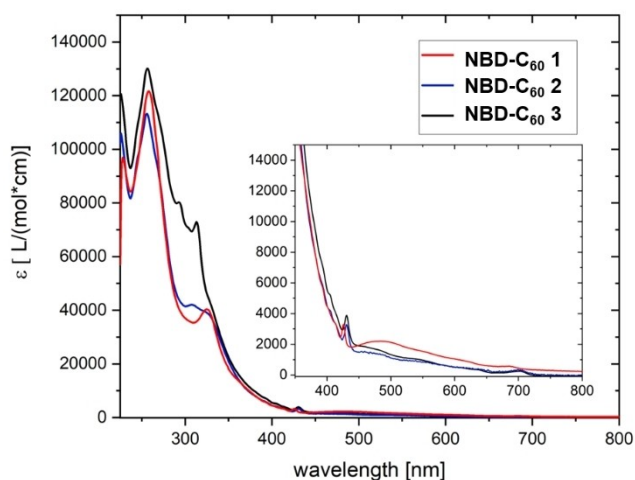


Figure 1. UV/vis absorption spectra of **NBD-C₆₀ 1–3** measured in CH_2Cl_2 . The inset highlights the absorption band around 430 nm.

observed since these are superimposed by the strong absorption of the fullerene core within the corresponding spectral region.

To gain more insight into the molecular structures and the interaction between the two building blocks we performed MD simulations in vacuum using the LAMMPS software package^[10] and the generalized Amber force field (GAFF).^[11] After an equilibration time of 50 ps, the molecules were kept at a constant temperature of 300 K using a Nose-Hoover thermostat for a simulation time of 50 ns. In Figure 2, the frequency distribution of the distance between the QC moieties center of mass and the respective fullerene core, derived from the trajectory every 100 fs, is shown. It is apparent that the molecular design of the linkers is ideal to realize NBD/QC – fullerene hybrids with varying distances between the two building blocks (Figure 2). The flexible linker in **QC-C₆₀ 1** results in close contact between the fullerene core and the QC moiety within the range of the van der Waals distance. For the short-rigid linker in **QC-C₆₀ 2**, a distance of around 11.4 Å is predominant. In contrast, the long-rigid linker in **QC-C₆₀ 3** allows for multiple orientations since the ethyl ester between the tolane and the QC moiety introduces some flexibility. However, the average distance between QC and fullerene core as determined over the whole simulation time is 14.2 Å and therefore the highest value of all three hybrids.

With **NBD-C₆₀ 1–3** and the structural information from the MD simulations at hand, we investigated the isomerization to the corresponding QC derivatives **QC-C₆₀ 1–3**. To ensure good

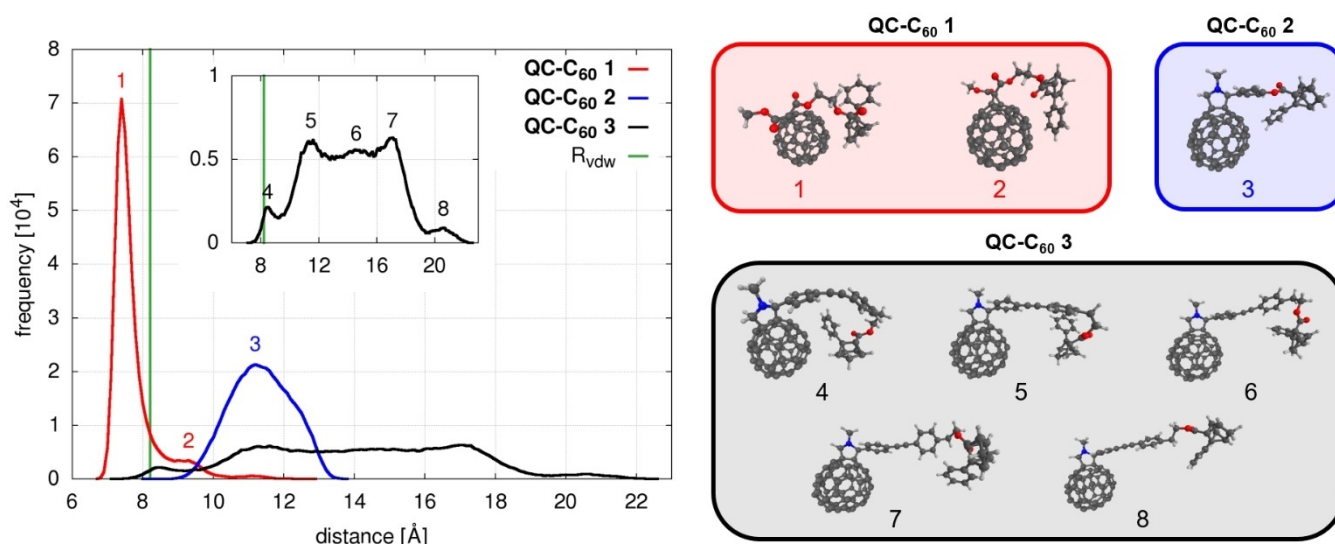


Figure 2. Left side: Histogram of the distance between the centers of mass of the QC moiety and the fullerene for the three QC – fullerene hybrids QC-C₆₀ 1–3, derived from the MD simulations. R_{vdw} is calculated as the sum of the van der Waals radius of a C₆₀ fullerene,^[12] the average distance of the carbon atoms of the QC moiety from the QC center of mass, and the van der Waals radius of a carbon atom.^[13] The numbers indicate the distances where representative structures were picked. Right side: Representative structures of QC-C₆₀ 1–3 during the MD simulation at the indicated distances.

comparability, an NMR tube was loaded with 1.0 mL of a 1.5×10^{-3} M solution of the respective NBD – fullerene hybrid dissolved in thoroughly degassed CDCl₃ and irradiated with a 310 nm UV-LED in a custom-made setup. In certain time intervals the NBD/QC ratio was determined by ¹H NMR spectroscopy and plotted against the irradiation time (Figure 3). As evident from Figure 3, full conversion (QC > 97%; determined from the integral ratio) from NBD to QC was observed for all three hybrids within five hours of irradiation. This is very

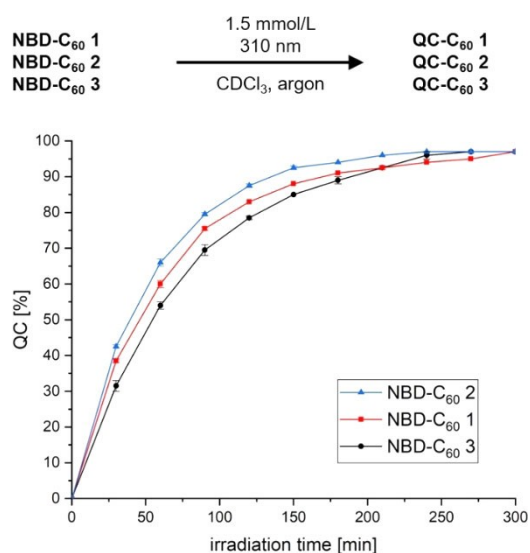


Figure 3. Photoisomerization of NBD-C₆₀ 1–3 to QC-C₆₀ 1–3 using a 310 nm UV-LED. The reaction was followed by ¹H NMR spectroscopy, the amount of formed QC was estimated from the integral ratio of QC/NBD. The average values of two distinct experiments including the standard deviation are depicted.

remarkable since, although the irradiation wavelength was matched with the absorption spectra of the incorporated push-pull NBDs (see Supporting Information), the fullerene core also absorbs light of this wavelength (see Figure 1).

Therefore, two competing reactions are to be expected. Because QC-C₆₀ 1–3 are formed, it can be concluded that the isomerization of NBD to QC is much more efficient than the competing back-reaction within these hybrids. Furthermore, the similar conversion efficiency observed for all three hybrids suggests that the nature of the linker has no significant influence on this reaction. The slightly faster isomerization of NBD-C₆₀ 2 most likely results from the different push-pull NBD that is incorporated in this hybrid. This can be explained by the slightly higher extinction coefficient as well as the broader absorption of this push-pull system compared to the one that is implemented in NBD-C₆₀ 1 and NBD-C₆₀ 3 (see Figure S17 in the Supporting Information). With the QC – fullerene hybrids QC-C₆₀ 1–3 at hand, the next step was the investigation of the light-induced back-reaction. Therefore, the very same NMR tubes used in the previous experiment were now irradiated with a 400 nm UV-LED in our custom-made setup. The reaction progress was again followed by ¹H NMR spectroscopy over a timespan of five hours and the amount of consumed QC was determined from the integral ratio of QC and NBD (Figure 4).

A pronounced difference in the rates of the back-reactions can be observed for the three hybrids QC-C₆₀ 1–3. The fastest back-reaction is observed for QC-C₆₀ 1 (flexible linker), with only 33% of QC-C₆₀ 1 remaining after five hours. In our earlier publication we showed already that this reaction can be driven to completion.^[7a] In contrast, the back-reaction of QC-C₆₀ 3 (long-rigid linker) to NBD-C₆₀ 3 proceeds much slower and after five hours still 87.5% of the QC derivative remain unconverted. In case of QC-C₆₀ 2 (short-rigid linker), the back-reaction

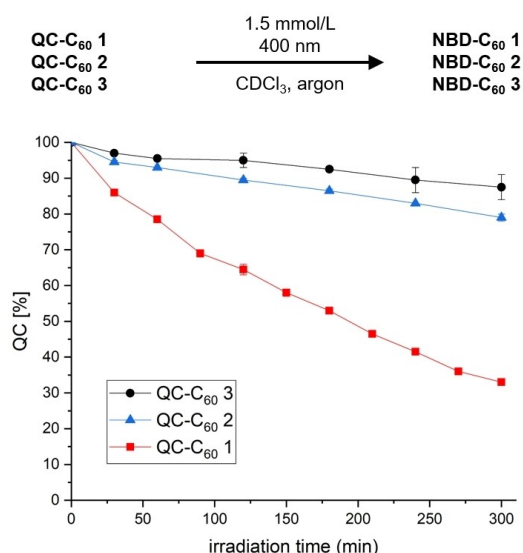


Figure 4. Photoisomerization of QC-C₆₀ 1–3 to NBD-C₆₀ 1–3 using a 400 nm UV-LED. The reaction was followed by ¹H NMR spectroscopy, the amount of consumed QC was estimated from the integral ratio of QC/NBD. The average values of two distinct experiments including the standard deviation are depicted.

proceeds also slowly, yet slightly faster than that of QC-C₆₀ 3 with 79% of QC-C₆₀ 2 remaining after the irradiation time of five hours. However, these values of QC-C₆₀ 2 have to be treated carefully since a control experiment in which NBD-C₆₀ 1–3 were irradiated with the 400 nm UV-LED under the same experimental conditions showed some formation of QC-C₆₀ 2, whereas no formation of QC-C₆₀ 1 and QC-C₆₀ 3 was observed (see Figures S13–S15 and Table S7 in the Supporting Information). This can be explained by the slightly different NBD moiety incorporated in QC-C₆₀ 2. QC-C₆₀ 1/3 both feature the same push-pull substituted NBD scaffold, namely a phenyl ring as the electron donating group (EDG) and an ethyl ester as the EWG. In contrast, QC-C₆₀ 2 features a *para*-substituted phenyl ester instead of the ethyl ester. By synthesizing and comparing these ‘isolated’ NBD derivatives we were able to show that this slight variation of the EWG causes a red-shift of the absorption profile of the respective NBD band (Supporting Information, Figure S17). Because of that, the NBD moiety of NBD-C₆₀ 2 is prone to excitation with the 400 nm UV-LED and thus isomerization to the corresponding QC-C₆₀ 2 is observed (see Table S8 and Figure S18 in the Supporting Information). In case of the back-reaction QC-C₆₀ 2 to NBD-C₆₀ 2, two competing reactions run simultaneously, causing the rate of this back-reaction to be underestimated in Figure 4. Nevertheless, since no isomerization of NBD-C₆₀ 1/3 was observed under irradiation with the 400 nm UV-LED, a good estimate of the influence of the linker on this back-reaction is possible. From the MD simulations the average distance between fullerene core and QC scaffold was determined and the rate of the back-reaction is in line with these observations, whereby greater distance results in a slower reaction. Several conclusions can be drawn from this, 1) the fullerene is definitely involved in the back-reaction, 2) close

contact between the two building blocks is a prerequisite, 3) within the investigated concentration regime an intramolecular mechanism is predominant, 4) the photoisomerization NBD to QC via irradiation of the push-pull substituted NBD systems is much more efficient than the back-reaction involving the fullerene core. In our previous publication we proposed that C₆₀ acts as an excited state electron acceptor that oxidizes QC and thus initiates the back-reaction.^[7a] This hypothesis is further strengthened not only by the observations made in this study but also by calculating the HOMOs and LUMOs of the QC – fullerene hybrids (Figure 5 and Supporting Information). According to these calculations, the LUMO is exclusively located on the fullerene core, which is in line with the expectations. This, in combination with the fact that QC is one of, if not the easiest to oxidize saturated hydrocarbons,^[14] further substantiates our proposed mechanism.

Conclusion

In conclusion, by careful molecular design it was possible to tune the average distance between fullerene core and photo-switch in the range of 7.8 Å in QC-C₆₀ 1 and 14.2 Å in QC-C₆₀ 3. This not only allowed us to gain valuable insight into the interaction of these two building blocks, but also provides a tool to control the back-reaction. This, in combination with the observation that slight variations of the incorporated push-pull substituted NBD moiety also have a pronounced impact on the system, renders NBD/QC – fullerene hybrids highly tunable systems with the possibility to achieve tailor-made photo-switches.

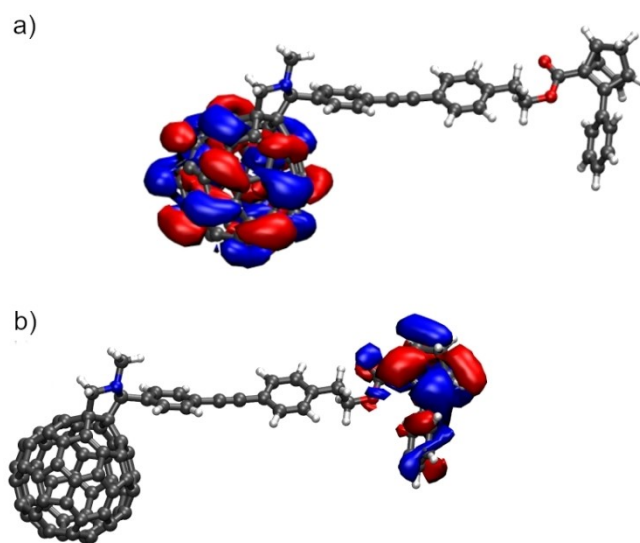


Figure 5. Frontier molecular orbitals, a) LUMO and b) HOMO of QC-C₆₀ 3 (isovalue 0.0128 au).

Experimental Section

NBD-C₆₀ 1: The preparation as well as the ¹H and ¹³C NMR spectra of **NBD-C₆₀ 1** has already been reported in our earlier publication.^[7a] All spectroscopic data were in agreement with those previously published. M.p. thermal decomposition (TLC analysis of the left-over material after heating **NBD-C₆₀ 1** to 360 °C indicated decomposition).

NBD-C₆₀ 2: Compound **4** (71.0 mg, 1.00 equiv., 8.16 × 10⁻⁵ mol) was dissolved in *ortho*-dichlorobenzene (25 mL) under inert atmosphere. Successively, **NBD-acid 5** (19.1 mg, 1.10 equiv., 8.98 × 10⁻⁵ mol), DCC (18.5 mg, 1.10 equiv., 8.98 × 10⁻⁵ mol) and DMAP (2.0 mg, 0.20 equiv., 1.6 × 10⁻⁵ mol) were added and the reaction mixture was stirred at room temperature overnight. After that time, the reaction mixture was directly transferred to column chromatography on SiO₂ using a mixture of toluene/ethyl acetate 9/1 v:v as eluent. The product was obtained as a brown powder after precipitation from CS₂ with *n*-pentane. (Mixture of diastereomers and enantiomers see Supporting Information) Yield: 42.0 mg, 3.95 × 10⁻⁵ mol, 48%. M.p. thermal decomposition (TLC analysis of the left-over material after heating **NBD-C₆₀ 2** to 360 °C indicated decomposition). ¹H NMR (600 MHz, CDCl₃) δ = 7.84–7.73 (bs, 2H), 7.58–7.56 (m, 2H), 7.35–7.28 (m, 3H), 7.15–7.14 (m, 2H), 7.05–6.95 (m, 2H), 4.99–4.97 (m*, 1H), 4.93 (m*, 1H), 4.27 (d*, 1H), 4.20–4.19 (m, 1H), 3.92–3.91 (m, 1H), 2.81 (s*, 3H), 2.36–2.34 (m, 1H), 2.17–2.15 (m, 1H) ppm. *for these signals, due to the presence of diastereomers (see Supporting Information), a second signal set is observed. ¹³C NMR (151 MHz, CDCl₃) δ = 169.6, 162.8, 156.1, 153.9, 153.2, 153.0, 150.8, 147.3, 147.2, 146.6, 146.4, 146.3, 146.2, 146.2, 146.1, 146.1, 146.1, 146.1, 145.9, 145.9, 145.7, 145.5, 145.5, 145.5, 145.4, 145.3, 145.3, 145.3, 145.2, 145.2, 145.2, 145.1, 144.7, 144.6, 144.4, 144.3, 143.7, 143.1, 143.0, 142.7, 142.6, 142.5, 142.5, 142.2, 142.2, 142.1, 142.1, 142.1, 142.0, 142.0, 142.0, 141.9, 141.8, 141.7, 141.5, 141.5, 140.6, 140.2, 140.1, 139.9, 139.9, 139.6, 138.1, 136.9, 136.5, 135.8, 135.7, 135.3, 133.9, 130.0, 129.0, 128.0, 127.8, 121.9, 83.0, 70.6, 70.0, 68.9, 59.0, 53.3, 40.0 ppm. HRMS (APPI, CH₂Cl₂) [M + H]⁺ m/z = 1064.1645 (calcd.), 1064.1631 (found).

NBD-C₆₀ 3: Compound **7** (135 mg, 1.00 equiv., 1.35 × 10⁻⁴ mol) was dissolved in CH₂Cl₂ (150 mL) under inert atmosphere. Successively, **NBD-acid 5** (57.5 mg, 2.00 equiv., 2.71 × 10⁻⁴ mol), DCC (80.0 mg, 2.87 equiv., 3.88 × 10⁻⁴ mol) and DMAP (13.2 mg, 0.800 equiv., 1.08 × 10⁻⁴ mol) were added and the reaction mixture was stirred and heated to reflux over three days. After that time, reaction control by TLC showed only insufficient conversion, therefore, more **NBD-acid 5** (43.0 mg, 1.50 equiv., 2.03 × 10⁻⁴ mol), DCC (60.0 mg, 2.15 equiv., 2.91 × 10⁻⁴ mol) and DMAP (9.9 mg, 0.60 equiv., 8.1 × 10⁻⁵ mol) were added and stirring and heating were continued for further 11 days. Afterwards the reaction mixture was concentrated and purified by column chromatography on SiO₂ using a mixture of toluene/ethyl acetate 9/1 v:v as eluent. The product was obtained as a brown powder after precipitation from CS₂ with *n*-pentane. (Mixture of diastereomers and enantiomers see Supporting Information) Yield 25.0 mg, 2.10 × 10⁻⁵ mol, 16%. M.p. thermal decomposition (TLC analysis of the left-over material after heating **NBD-C₆₀ 3** to 360 °C indicated decomposition). ¹H NMR (600 MHz, CDCl₃) δ = 7.81 (bs, 2H), 7.60–7.59 (m, 2H), 7.48–7.46 (m, 2H), 7.41–7.39 (m, 2H), 7.35–7.29 (m, 3H), 7.09–7.07 (m, 2H), 6.94–6.89 (m, 2H), 5.00 (d, J = 9.4 Hz, 1H), 4.95 (s, 1H), 4.30–4.27 (m, 3H), 4.01–4.00 (m, 1H), 3.84–3.83 (m, 1H), 2.89 (t, J = 6.8 Hz, 2H), 2.82 (s, 3H), 2.24–2.22 (m, 1H), 2.05–2.04 (m, 1H) ppm. ¹³C NMR (151 MHz, CDCl₃) δ = 167.4, 165.4, 156.3, 154.1, 153.4, 153.2, 147.5, 146.8, 146.6, 146.5, 146.4, 146.4, 146.3, 146.3, 146.3, 146.2, 146.1, 146.1, 145.9, 145.7, 145.7, 145.6, 145.5, 145.5, 145.5, 145.4, 145.4, 145.3, 144.9, 144.8, 144.6, 144.5, 143.8, 143.3, 143.3, 143.2, 142.9, 142.8, 142.7, 142.7, 142.4, 142.4, 142.3, 142.3, 142.3, 142.2, 142.2, 142.1, 142.0, 141.9, 141.7, 141.0, 140.4, 140.3, 140.1, 139.8, 139.1, 138.8, 137.4, 137.0, 136.6,

136.1, 135.9, 135.9, 132.0, 131.8, 129.5, 129.1, 128.7, 127.9, 127.9, 123.6, 121.3, 90.2, 89.1, 83.5, 70.7, 70.2, 69.2, 64.4, 58.8, 53.1, 40.2, 35.1 ppm. HRMS (MALDI-TOF, DCTB) [M]⁻ m/z = 1191.2198 (calcd.), 1191.2193 (found).

General procedure for the synthesis of QC-C₆₀ 1–3: For the preparation of **QC-C₆₀ 1–3**, an NMR tube was charged with 1.00 mL of a 1.50 × 10⁻³ M solution of the respective NBD – fullerene hybrid dissolved in thoroughly (pump-freeze-thaw) degassed CDCl₃ under argon atmosphere in the glovebox. The tube was sealed, removed from the glovebox and irradiated with a 310 nm UV-LED in a custom-made setup until no further change was observed in the ¹H NMR spectrum (approx. 5 h).

QC-C₆₀ 1: The preparation as well as the ¹H and ¹³C NMR spectra of **QC-C₆₀ 1** has already been reported in our earlier publication.^[7a] All spectroscopic data were in agreement with those previously published.

QC-C₆₀ 2: ¹H NMR (600 MHz, CDCl₃) δ = 7.72 (bs, 2H), 7.33–7.31 (m, 2H), 7.28–7.25 (m, 2H), 7.19–7.16 (m, 1H), 7.06–7.05 (m, 2H), 4.96 (d, J = 9.4 Hz, 1H), 4.88 (s, 1H), 4.23 (d, J = 9.4 Hz, 1H), 2.80–2.78 (m, 1H), 2.75 (s, 3H), 2.70–2.68 (m, 1H), 2.48–2.46 (m, 1H), 2.33–2.32 (m, 1H), 2.23–2.21 (m, 1H), 1.79–1.77 (m, 1H) ppm. ¹³C NMR (151 MHz, CDCl₃) δ = 170.2, 156.4, 154.2, 153.5, 153.3, 150.7, 147.5, 146.8, 146.6, 146.5, 146.4, 146.4, 146.3, 146.3, 146.3, 146.1, 146.1, 145.9, 145.7, 145.7, 145.7, 145.6, 145.5, 145.5, 145.5, 145.4, 145.4, 145.3, 144.9, 144.7, 144.6, 144.5, 143.3, 143.1, 142.8, 142.7, 142.7, 142.7, 142.4, 142.4, 142.3, 142.3, 142.3, 142.2, 142.2, 142.1, 142.0, 141.8, 141.7, 140.3, 140.3, 140.1, 139.7, 137.0, 136.6, 136.0, 135.8, 134.1, 130.2, 128.8, 128.0, 126.5, 121.9, 83.2, 70.2, 69.2, 40.1, 38.5, 38.5, 33.1, 32.5, 32.5, 32.0, 31.8, 31.0, 31.0, 21.2 ppm.

QC-C₆₀ 3: ¹H NMR (600 MHz, CDCl₃) δ = 7.81 (bs, 2H), 7.61–7.59 (m, 2H), 7.39–7.37 (m, 2H), 7.26–7.23 (m, 4H), 7.20–7.17 (m, 1H), 6.98–6.96 (m, 2H), 5.00 (d, J = 9.3 Hz, 1H), 4.95 (s, 1H), 4.28 (d, J = 9.4 Hz, 1H), 4.16–4.13 (m, 2H), 2.82 (s, 3H), 2.73 (t, J = 6.7 Hz, 2H), 2.51–2.49 (m, 1H), 2.41–2.40 (m, 1H), 2.37–2.34 (m, 1H), 2.22–2.21 (m, 1H), 2.13–2.11 (m, 1H), 1.70–1.69 (m, 1H) ppm. ¹³C NMR (151 MHz, CDCl₃) δ = 172.1, 156.3, 154.1, 153.4, 153.2, 147.5, 146.8, 146.6, 146.5, 146.5, 146.4, 146.3, 146.3, 146.3, 146.2, 146.1, 146.1, 145.9, 145.7, 145.7, 145.6, 145.5, 145.5, 145.5, 145.4, 145.4, 145.3, 144.9, 144.8, 144.6, 144.5, 143.3, 143.3, 143.2, 142.9, 142.8, 142.7, 142.7, 142.4, 142.4, 142.3, 142.3, 142.3, 142.2, 142.2, 142.1, 142.0, 141.9, 141.7, 140.4, 140.3, 140.1, 139.8, 138.8, 137.4, 137.2, 137.0, 136.6, 136.1, 135.9, 132.0, 131.7, 129.5, 129.1, 128.9, 127.8, 126.4, 123.6, 121.2, 90.2, 89.1, 83.5, 70.2, 69.2, 64.2, 40.2, 37.5, 35.0, 33.0, 32.4, 31.8, 31.7, 29.7, 21.0 ppm.

Computational Methods

The MD simulations were performed using the LAMMPS software package^[10] and the generalized Amber force field (GAFF).^[11] London dispersion interactions were taken into account by pair-wise Lennard-Jones terms. After an equilibration time of 50 ps, the molecules were kept at a constant temperature of 300 K using a Nose-Hoover thermostat with a damping time of 10 fs. The overall simulation time was 50 ns with a time step of 1 fs. The frontier molecular orbitals were calculated using the ORCA program package^[15] at the B3LYP/def2-TZVP level of theory.

Acknowledgements

We gratefully thank the German Research Foundation (DFG) for funding through SFB 953 “Synthetic Carbon Allotropes”, GRK 2423 and project 391585168 “Photochemisch und magnetochemisch ausgelöste Speicherung/Freisetzung von Sonnenenergie in gespannten organischen Verbindungen”. Open Access funding enabled and organized by Projekt DEAL.

Conflict of Interest

The authors declare no conflict of interest.

Keywords: energy conversion · fullerenes · molecular switches · norbornadiene · photoswitch

- [1] a) J. Orrego-Hernández, A. Dreos, K. Moth-Poulsen, *Acc. Chem. Res.* **2020**, *53*, 1478–1487; b) C.-L. Sun, C. Wang, R. Boulatov, *ChemPhotoChem* **2019**, *3*, 268–283; c) K. Börjesson, A. Lennartson, K. Moth-Poulsen, *ACS Sustainable Chem. Eng.* **2013**, *1*, 585–590.
- [2] A. Lennartson, A. Roffey, K. Moth-Poulsen, *Tetrahedron Lett.* **2015**, *56*, 1457–1465.
- [3] a) A. D. Dubonosov, V. A. Bren, V. A. Chernov, *Russ. Chem. Rev.* **2002**, *71*, 917–927; b) V. A. Bren, A. D. Dubonosov, V. I. Minkin, V. A. Chernov, *Russ. Chem. Rev.* **1991**, *60*, 451–469.
- [4] a) F. Waidhas, M. Jevric, M. Bosch, T. Yang, E. Franz, Z. Liu, J. Bachmann, K. Moth-Poulsen, O. Brummel, J. Libuda, *J. Mater. Chem. A* **2020**, *8*, 15658–15664; b) F. Waidhas, M. Jevric, L. Fromm, M. Bertram, A. Görling, K. Moth-Poulsen, O. Brummel, J. Libuda, *Nano Energy* **2019**, *63*, 103872; c) O. Brummel, F. Waidhas, U. Bauer, Y. Wu, S. Bochmann, H.-P. Steinrück, C. Papp, J. Bachmann, J. Libuda, *J. Phys. Chem. Lett.* **2017**, *8*, 2819–2825; d) O. Brummel, D. Besold, T. Döpper, Y. Wu, S. Bochmann, F. Lazzari, F. Waidhas, U. Bauer, P. Bachmann, C. Papp, H.-P. Steinrück, A. Görling, J. Libuda, J. Bachmann, *ChemSusChem* **2016**, *9*, 1424–1432.
- [5] a) Z. Wang, A. Roffey, R. Losantos, A. Lennartson, M. Jevric, A. U. Petersen, M. Quant, A. Dreos, X. Wen, D. Sampedro, K. Börjesson, K. Moth-Poulsen, *Energy Environ. Sci.* **2019**, *12*, 187–193; b) Z. Yoshida, *J. Photochem.* **1985**, *29*, 27–40.
- [6] a) P. Lorenz, T. Luchs, A. Hirsch, *Chem. Eur. J.* **2021**, *27*, 4993–5002; b) T. Luchs, P. Lorenz, A. Hirsch, *ChemPhotoChem* **2020**, *4*, 52–58; c) U. Bauer, S. Mohr, T. Döpper, P. Bachmann, F. Späth, F. Düll, M. Schwarz, O. Brummel, L. Fromm, U. Pinkert, A. Görling, A. Hirsch, J. Bachmann, H.-P. Steinrück, J. Libuda, C. Papp, *Chem. Eur. J.* **2017**, *23*, 1613–1622; d) S. Miki, Y. Asako, M. Morimoto, T. Ohno, Z. Yoshida, T. Maruyama, M. Fukuoka, T. Takada, *Bull. Chem. Soc. Jpn.* **1988**, *61*, 973–981; e) S. Miki, T. Maruyama, T. Ohno, T. Tohma, S. Toyama, Z. Yoshida, *Chem. Lett.* **1988**, *17*, 861–864; f) J. Manassen, *J. Catal.* **1970**, *18*, 38–45.
- [7] a) P. Lorenz, A. Hirsch, *Chem. Eur. J.* **2020**, *26*, 5220–5230; b) B. E. Tebikachew, F. Edhborg, N. Kann, B. Albinsson, K. Moth-Poulsen, *Phys. Chem. Chem. Phys.* **2018**, *20*, 23195–23201; c) A. Dreos, Z. Wang, B. E. Tebikachew, K. Moth-Poulsen, J. Andréasson, *J. Phys. Chem. Lett.* **2018**, *9*, 6174–6178.
- [8] T. Cao, K. Chen, Q. Chen, Y. Zhou, N. Chen, Y. Li, *ACS Appl. Mater. Interfaces* **2019**, *11*, 33825–33834.
- [9] K. Kordatos, T. Da Ros, M. Prato, R. V. Bensasson, S. Leach, *Chem. Phys.* **2003**, *293*, 263–280.
- [10] S. Plimpton, *J. Comput. Phys.* **1995**, *117*, 1–19.
- [11] J. Wang, R. M. Wolf, J. W. Caldwell, P. A. Kollman, D. A. Case, *J. Comput. Chem.* **2004**, *25*, 1157–1174.
- [12] M. S. Dresselhaus, G. Dresselhaus, P. C. Eklund, *Science of fullerenes and carbon nanotubes*; Acad. Press, San Diego, **1996**.
- [13] A. Bondi, *J. Phys. Chem.* **1964**, *68*, 441–451.
- [14] P. G. Gassman, R. Yamaguchi, G. F. Koser, *J. Org. Chem.* **1978**, *43*, 4392–4393.
- [15] F. Neese, *WIREs Comput. Mol. Sci.* **2012**, *2*, 73–78.

Manuscript received: June 14, 2021

Accepted manuscript online: July 30, 2021

Version of record online: September 16, 2021